

Light-matter interaction in open cavities with dielectric stacks

Astghik Saharyan¹, Juan-Rafael Álvarez², Thomas H. Doherty², Axel Kuhn^{2,*} and Stéphane Guerin^{1†}

¹ *Laboratoire Interdisciplinaire Carnot de Bourgogne, CNRS UMR 6303, Université Bourgogne Franche-Comté, BP 47870, F-21078 Dijon, France.*

² *University of Oxford, Clarendon Laboratory, Parks Road, Oxford, OX1 3PU, UK*

(Dated: September 18, 2020)

We evaluate the exact dipole coupling strength between a single emitter and the radiation field within an optical cavity, taking into account the effects of multilayer dielectric mirrors. Our model allows one to freely vary the resonance frequency of the cavity, the frequency of light or atomic transition addressing it and the design wavelength of the dielectric mirror. The coupling strength is derived for an open system with unbound frequency modes. For very short cavities, the effective length used to determine their mode volume and the lengths defining their resonances are different, and also found to diverge appreciably from their geometric length, with the radiation field being strongest within the dielectric mirror itself. Only for cavities much longer than their resonant wavelength does the mode volume asymptotically approach that normally assumed from their geometric length.

I. INTRODUCTION

The development of universal quantum computation remains a key endeavour in the coherent control and manipulation of quantum states of light and matter. A principal component of this effort is improving the inherent scalability of current architectures; developing methods for the reliable interconnection of distant qubits and quantum processors [1]. A promising approach is the use of high finesse optical cavities to couple individual states of light and matter, thereby proving a bridge between stationary emitters and travelling photons as the hosts of quantum information. A strong coupling within the cavity allows this to be a controllable, deterministic and inherently reversible interaction, essentially establishing an idealised quantum interface [2, 3]. In principle, this allows for the generation of light-matter entanglement [4], entanglement swapping [5] and the distribution of cluster states over an extended quantum network [6]. In the short term, similar systems have been used extensively for the enhanced production of single photons, across a variety of emitter types and platforms such as neutral atoms [7], ions [8], NV centers [9] and quantum dots [10].

All cavity mediated light-matter coupling schemes developed to date are based on the Purcell effect, which describes an enhancement to the spontaneous emission rate of a quantised emitter within a resonant cavity. When compared to isotropic spontaneous emission into free space, the rate of emission into the cavity mode is enhanced by the factor [11]:

$$F_p = \frac{3\lambda^3 Q}{4\pi^2 V}, \quad (1)$$

where Q is the quality factor of the resonator, λ is the transition wavelength and V is the optical mode volume of the resonator. In cavity QED systems which consider coupling to only a single emitter, this factor is commonly expressed as system cooperativity, given by $2C = F_p = g^2/(\kappa\gamma)$, where g is the atom-cavity coupling rate, κ is the cavity field decay rate and 2γ is the rate of atomic spontaneous emission. Strongly coupled systems are correspondingly defined as those where $g \gg (\kappa, \gamma)$, i.e., where the coherent coupling rate surpasses incoherent decay mechanisms [12]. The suppression of photonic decay within the cavity generally requires the use of highly reflective mirrors, characterised by a large cavity finesse, $\mathcal{F} = \pi\sqrt{R}/(1-R)$ [13], where R is the mirror reflectivity. Given the equivalent representation of finesse as the ratio of cavity free spectral range to its linewidth, a high finesse additionally ensures good spectral resolution of each resonance. Therefore, when an emitter with a comparable transition linewidth is coupled to a high finesse cavity, interaction with only a single field mode can be assumed.

To achieve the mirror reflectivity required for coherent atom-cavity interactions, highly reflective dielectric coatings, or Bragg stacks are used as standard [14]. These comprise layer pairs of quarter-wavelength optical thickness dielectric material, with alternating refractive indices. Generally, a high reflectivity is only achieved for a large number of such

*Electronic address: axel.kuhn@physics.ox.ac.uk

†Electronic address: sguerin@u-bourgogne.fr

layers, implying a notable penetration of the stack by incident light. A common strategy for enhancing cooperativity is the minimisation of mode volume, which generally requires reducing mirror spacing. At its extreme, the mirror spacing can be of the same order as the resonant wavelength of interest [15]. This unintentionally increases the relative portion of the cavity mode within the dielectric stack [14, 16, 17], rendering the standard optical models of a Fabry-Pérot resonator inaccurate. The propagation of light in dielectric stacks has been studied before under resonance conditions [14, 17, 18]. Here we go a step further in considering the more general case of a wave of arbitrary wavelength traveling through the stack. Note that this is always the case if the emitter coupled to the cavity is not resonant with the cavity mode.

In order to model the dynamics within a cavity, the quantized light field is normalized in terms of its quantization volume, which normally corresponds to the geometric volume of the optical resonator [19]. However, in the case of the ultra-strong coupling resonator we consider here, modelling the surface of the mirror as a hard boundary to the cavity mode is no longer appropriate. To rectify this, we consider an open cavity system, where the electric field is able to propagate through the dielectric mirror and couples to external free-space modes. This departs from the standard notion of having a mode volume and well defined frequency modes of the resonator, suitably modifying our calculation of the Purcell Factor. Whilst some aspects have already been addressed in the past, [20, 21], a description which takes into account a large number of dielectric layers has not been reported, and only the resonant case where the field has the design wavelength of the dielectric stacks.

In this paper we revise the concept of mode volume and cavity resonance frequency for a cavity formed from dielectric mirrors. In Section 2 we describe the general quantisation procedure to be used for an atom within a cavity, where it interacts with a global electromagnetic field. This procedure departs from the standard input-output formulation used in the existing literature reporting open optical systems [19, 22, 23]. From this, we obtain a general expression for the coupling strength between the field and atom. As a reasonable approximation, we consider a cavity which consists of one perfectly reflective mirror and one partially transparent mirror of finite thickness. At the beginning of Section 3 we model the partially-transparent cavity mirror as a single dielectric slab, a case that has been considered extensively in associated literature [19, 22]. Then, we expand it into a multilayer stack, repeating our analysis. This allows for a discussion on a more realistic specification of effective cavity length and corresponding mode volume for short cavities. We show that the expected resonance frequency of the cavity, the resonant frequency of the emitter and the design frequency of the dielectric stack may differ substantially from one another. By considering the boundary to these effects, we demonstrate that the standard models of optical resonance are asymptotically re-achieved at extended cavity lengths. Finally, in Section 4 we develop a new model for calculating the coupling of an emitter to this light field, modelled as an open quantum system and unconstrained by the surface of the mirrors.

II. ATOM-FIELD COUPLING

The electromagnetic field within a cavity is described by solution of the Helmholtz equation:

$$\left(\frac{d^2}{dx^2} + \epsilon_r(x) \frac{\omega^2}{c^2} \right) \Phi_\omega(x) = 0, \quad (2)$$

where $\epsilon_r(x)$ is the relative permittivity of the physical medium, $\Phi_\omega(x)$ is the space-dependent field eigenmode of continuous index $\omega = 2\pi c/\lambda$, where λ is the wavelength of the travelling wave and c is the speed of light. The orthonormalization condition for these modes is given by:

$$\langle \Phi_\omega, \Phi_{\omega'} \rangle = \int_{-\infty}^{\infty} dx \epsilon_r(x) \Phi_\omega^*(x) \Phi_{\omega'}(x) = \delta(\omega - \omega'). \quad (3)$$

For convenience, eigenmodes can be spatially separated into three regions: between the mirrors, within the stack, and outside of the cavity:

$$\Phi_\omega(x) = \Phi_{\omega,\text{in}}(x) + \Phi_{\omega,\text{stack}}(x) + \Phi_{\omega,\text{out}}(x). \quad (4)$$

The corresponding quantized electric field can be written in the Schrödinger picture as:

$$\hat{E}(x) = -i \int_0^\infty d\omega \sqrt{\frac{\hbar\omega}{2\epsilon_0}} (\Phi_\omega(x) \hat{a}_\omega - \Phi_\omega^*(x) \hat{a}_\omega^\dagger), \quad (5)$$

where

$$\begin{aligned} [\hat{a}_\omega, \hat{a}_{\omega'}^\dagger] &= \delta(\omega - \omega'), \\ [\hat{a}_\omega, \hat{a}_{\omega'}] &= 0. \end{aligned}$$

We highlight that the above quantization procedure from first principles does not break the modes into separate parts (as opposed to any approach first quantizing the field inside a perfect cavity and subsequently coupling the field modes to the outside using a variety of input-output formalisms [22, 23]), but rather considers the global modes occupying all the Hilbert space. These global modes behave as uncoupled quantum harmonic oscillators with a Hamiltonian of the form:

$$\hat{H} = \int_0^\infty d\omega \hbar\omega \left(\hat{a}_\omega^\dagger \hat{a}_\omega + \frac{1}{2} \right),$$

where the $1/2$ term is usually removed by renormalizing the zero-point energy of the field.

To take into account the interaction of the field with an atom localized between the mirrors, one would like:

1. To derive an effective Hamiltonian and master equations accounting for the dynamics inside of the cavity;
2. To describe the leakage of the photons from the cavity;
3. To characterize the photons leaking out of the cavity.

For which two strategies can be applied:

1. Deriving the approximate field Hamiltonians inside and outside the cavity *before* introducing the atom [22], which is then coupled to the Hamiltonian within the cavity;
2. Deriving approximate Hamiltonians where the atom is included in the cavity initially.

We focus on the second strategy because we are interested in finding the most accurate description of emitter-cavity coupling. The presence of the atom from the outset makes the calculations relatively simpler to those of [22], since the atom, localized in space and interacting with the global modes \hat{a}_ω , leads to a mode-selective behavior of the overall system.

Let us assume that a point-like two-level atom with states $|g\rangle$ and $|e\rangle$ separated in energy by $\hbar\omega_A$, is positioned at $x = x_A$, between a perfect, mirror placed at $x = -\ell_c$ and a partially transparent dielectric mirror positioned at the origin. Here, $-\ell_c < x_A < 0$, where ℓ_c is the geometric length of the cavity. The electric field at the position of the atom can be written by evaluating Eq. (5) at $x = x_A$, and we consider a field-atom dipolar interaction:

$$\hat{V} = -\hat{d}\hat{E}(x_A),$$

where $\hat{d} = d\hat{\sigma}_+ + d^*\hat{\sigma}_-$ is the dipole moment of the atom, $\hat{\sigma}_+ = |e\rangle\langle g|$ and $\hat{\sigma}_- = |g\rangle\langle e|$. By applying the rotating wave approximation, the interaction terms read:

$$\hat{V} = i\hbar \int_0^{+\infty} d\omega (\eta_\omega \hat{\sigma}_+ \hat{a}_\omega - \eta_\omega^* \hat{a}_\omega^\dagger \hat{\sigma}_-),$$

with a coupling strength given by:

$$\eta_\omega = \sqrt{\frac{\omega}{2\hbar\epsilon_0}} d \Phi_{\omega,\text{in}}(x_A). \quad (6)$$

Therefore, the total Hamiltonian of the atom-cavity global system is of the form

$$\hat{H} = \hbar\omega_A \hat{\sigma}_+ \hat{\sigma}_- + \int_0^{+\infty} d\omega \hbar\omega \hat{a}_\omega^\dagger \hat{a}_\omega + i\hbar \int_0^{+\infty} d\omega (\eta_\omega \hat{\sigma}_+ \hat{a}_\omega - \eta_\omega^* \hat{a}_\omega^\dagger \hat{\sigma}_-), \quad (7)$$

where the first term corresponds to the energy of the atom, the second term to the energy of the global electromagnetic field and the third term the interaction of this field with the atom placed between the mirrors.

In order to derive an effective Hamiltonian describing the dynamics of the open atom-cavity system, we need to derive an effective atom-cavity coupling strength from Eq. (6). Therefore, it is necessary to find the modes Φ_ω that satisfy the orthonormalization condition Eq. (3). We perform this calculation, taking into account the structure of the partially transparent mirror of the cavity, in the following section.

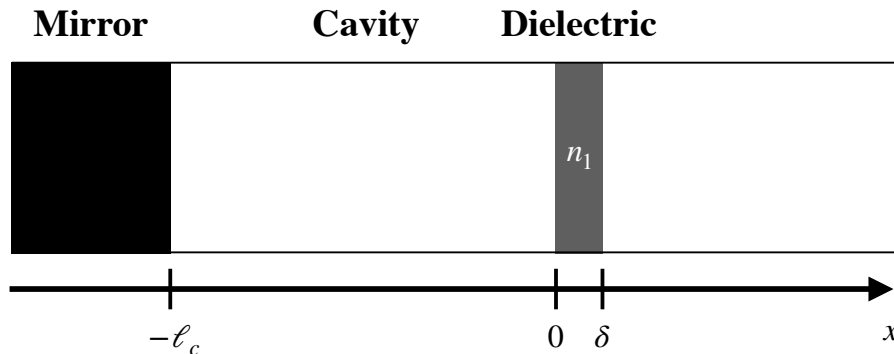


FIG. 1: Description of the single-layered cavity model. A perfect mirror stands at $x = -\ell_c$, delimiting a cavity of length ℓ_c with a partially transparent dielectric material from $x = 0$ to $x = \delta$.

III. FIELD MODES IN BRAGG STACKS

We first review the propagation of light in a cavity with a thin single-layered mirror and then build upon it to describe the case of multilayered stacks. Although this procedure is standard in the literature, it will prove important to show explicitly the differences that arise from realistic mirror structures. To ease calculation, we assume that the electromagnetic field between the mirrors can be separated into the product of a longitudinal and transverse component [24] and only consider the longitudinal propagation in the following.

A. Important parameters

For the purposes of future reference, we list here the parameters used to characterise our system in the following sections.

Definition	Notation
Mirror stack design wavelength and angular frequency.	$\lambda_0, \omega_0 = \frac{2\pi c}{\lambda_0}$
Propagating light wavelength and angular frequency (continuous).	$\lambda, \omega = \frac{2\pi c}{\lambda}$
Geometric cavity length, cavity resonance wavelength and angular frequency.	$\ell_c, \lambda_m, \omega_m = \frac{2\pi c}{\lambda_m} = \frac{\pi c m}{\ell_c}$
Actual cavity resonance angular frequency, leading to a resonance effective length.	$\omega_{\text{eff}} = \omega_N^{(m)}, \ell_{\text{eff}} = \frac{\pi c m}{\omega_{\text{eff}}}$
Coupling factor cavity length.	$L_N^{(m)}$

TABLE I: Relevant notations for the different wavelengths and frequencies within the atom-cavity system. The index m corresponds to the number of anti-nodes of the wave between the mirrors, and N to the $2N - 1$ dielectric layers.

B. Single-layered stack

Let us model a cavity of length ℓ_c . For the sake of simplicity, we assume that such a cavity has a perfect mirror on the left side, positioned at $x = -\ell_c$, and a partially transparent dielectric placed at the origin, with a refractive index n_1 and a thickness δ . The dielectric layer thickness has been designed to support a target wavelength, λ_0 . This structure can be seen in Fig. 1. In this structure, the spatial distribution of the electromagnetic field mode $\Phi_\omega(x)$ with frequency $\omega = 2\pi c/\lambda$ is described by the Helmholtz equation (2), with a relative permittivity structure of the form

$$\epsilon_r(x) = \begin{cases} 1 & x \in [-\ell_c, 0] \cup [\delta, \infty) \\ n_1^2 & x \in (0, \delta) \end{cases}.$$

Under these conditions, Helmholtz's equation is solved by a superposition of plane waves of the form

$$\Phi_\omega(x) = A_+ e^{i\frac{\omega}{c}\sqrt{\epsilon_r(x)}x} + A_- e^{-i\frac{\omega}{c}\sqrt{\epsilon_r(x)}x}.$$

The distinct solutions are then stitched together by the condition that $\Phi_\omega(x)$ and its derivative must ensure continuity throughout the points of discontinuity of $\epsilon_r(x)$, thus fixing the values of the coefficients A_+ and A_- for every region. For a single-layered stack, the solution has the form

$$\Phi_\omega(x) = \Phi_{\omega,\text{in}}(x)\chi_{[-\ell_c,0]} + \Phi_{\omega,\text{stack}}(x)\chi_{(0,\delta)} + \Phi_{\omega,\text{out}}(x)\chi_{[\delta,\infty)}, \quad (8)$$

following the convention defined by Eq. (4). Here, $\chi_{\mathcal{D}}$ represents the indicator function within a domain $\mathcal{D} \subset \mathbb{R}$, i.e., $\chi_{\mathcal{D}}(x) = 1$ for $x \in \mathcal{D}$ and 0 otherwise. The normalized mode is described in the three regions by:

$$\begin{aligned} \Phi_{\omega,\text{in}}(x) &= \frac{2i}{\sqrt{2\pi c\mathcal{A}}} e^{i\frac{\omega}{c}\ell_c} T(\omega) \sin\left[\frac{\omega}{c}(x + \ell_c)\right], \\ \Phi_{\omega,\text{stack}}(x) &= \frac{1}{\sqrt{2\pi c\mathcal{A}}} e^{i\frac{\omega}{c}\ell_c} \frac{T(\omega)}{1+r_1} [(e^{i\frac{\omega}{c}\ell_c} - r_1 e^{-i\frac{\omega}{c}\ell_c}) e^{i\frac{\omega}{c}n_1x} + (r_1 e^{i\frac{\omega}{c}\ell_c} - e^{-i\frac{\omega}{c}\ell_c}) e^{-i\frac{\omega}{c}n_1x}], \\ \Phi_{\omega,\text{out}}(x) &= \frac{1}{\sqrt{2\pi c\mathcal{A}}} e^{2i\frac{\omega}{c}\ell_c} \frac{T(\omega)}{T^*(\omega)} e^{i\frac{\omega}{c}x} - e^{-i\frac{\omega}{c}x}, \end{aligned} \quad (9)$$

where \mathcal{A} is the transverse area of the mode (a quantity which is calculated when the mode is normalized in three dimensions.), and r is the single-layer reflectivity

$$r_1 = \frac{n_1 - 1}{n_1 + 1},$$

$T(\omega)$ is the cavity spectral response function, which describes the ratio of intensity between the inside and outside of the cavity, with respect to a particular frequency ω :

$$T(\omega) = \frac{t(\omega)}{1 + r(\omega)e^{2i\frac{\omega}{c}(\ell_c + \frac{\delta}{2})}}. \quad (10)$$

It depends on the cavity spectral transmission response function $t(\omega)$ [19]:

$$t(\omega) = \frac{(1 - r_1^2)e^{i(n_1-1)\frac{\omega}{c}\delta}}{1 - e^{2in_1\frac{\omega}{c}\delta}r_1^2},$$

and spectral reflection response function $r(\omega)$:

$$r(\omega) = e^{-i\frac{\omega}{c}\delta} \frac{r_1(e^{2in_1\frac{\omega}{c}\delta} - 1)}{1 - e^{2in_1\frac{\omega}{c}\delta}r_1^2} = |r(\omega)| e^{i\phi_r(\omega)}.$$

It is important to stress that both of these parameters are complex and have associated phases. We will use $\phi_r(\omega)$ in later sections. Together, $t(\omega)$ and $r(\omega)$ satisfy the beam splitter relations

$$|t(\omega)|^2 + |r(\omega)|^2 = 1, \quad (11)$$

$$r^*(\omega)t(\omega) + t^*(\omega)r(\omega) = 0. \quad (12)$$

The squared norm of the cavity response function can be decomposed as a sum of Lorentzian-like functions[19, 25], still having $\tilde{\omega}_m$ and γ_1 depending on ω : (see the details in Appendix A):

$$|T(\omega)|^2 = \sum_{m=-\infty}^{\infty} \frac{c}{2L_1} \frac{\gamma_1(\omega)}{(\omega - \tilde{\omega}_m(\omega))^2 + \left(\frac{\gamma_1(\omega)}{2}\right)^2}, \quad (13)$$

where

$$\begin{aligned} \gamma_1(\omega) &= -\frac{c}{L_1} \ln |r(\omega)|, \\ \tilde{\omega}_m(\omega) &= m\frac{\pi c}{L_1} + \frac{c}{2L_1} (\pi - \phi_r(\omega)), \\ L_1 &= \ell_c + \frac{\delta}{2}, \end{aligned} \quad (14)$$

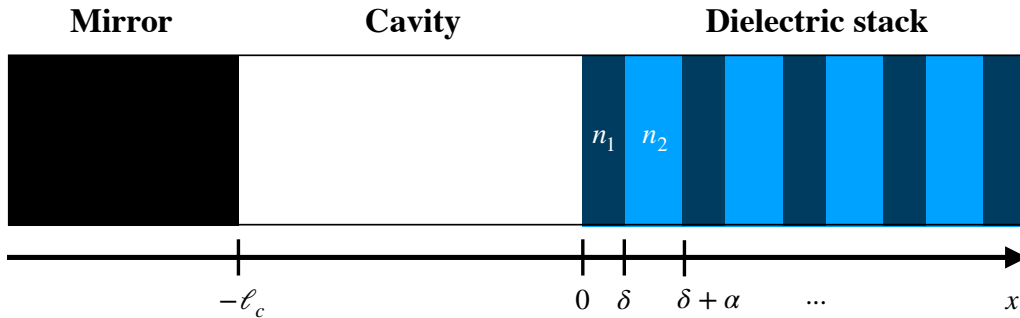


FIG. 2: Description of the considered model. A perfect mirror stands at $x = -\ell_c$, delimiting a cavity of length ℓ with an alternating dielectric stack standing from zero.

and index 1 in L_1 and γ_1 indicates that they are for the case of a single-layer mirror.

In the high- Q limit (reached when assuming a fictitious dielectric with a high refractive index), and for cavities having $\delta \ll \ell_c$, such that $L_1 \approx \ell_c$, the squared norm of the response function can be approximated as follows:

$$|T(\omega)|^2 \approx \sum_{m=-\infty}^{\infty} \frac{c}{2\ell_c} \frac{\Gamma_m}{(\omega - \tilde{\omega}_m)^2 + \left(\frac{\Gamma_m}{2}\right)^2}, \quad (15)$$

where

$$\Gamma_m = \gamma_1(\omega_m) = -\frac{c}{\ell_c} \ln |r(\omega_m)|, \quad (16)$$

$$\tilde{\omega}_m = \omega_m + \frac{c}{2\ell_c} (\pi - \phi_r(\omega_m)), \quad (17)$$

with $\omega_m = m\pi c/\ell_c$.

At this stage, the terms in the sum in Eq. (15) become Lorentzian, with each term centered around the resonance frequency $\tilde{\omega}_m$ and well separated from each other. Taking this into account we can now write the cavity response function as

$$T(\omega) \approx \sum_{m=-\infty}^{\infty} \sqrt{\frac{c}{2\ell_c}} \frac{\sqrt{\Gamma_m}}{(\omega - \tilde{\omega}_m) + i\frac{\Gamma_m}{2}} = \sum_{m=-\infty}^{\infty} T_m(\omega), \quad (18)$$

where $T_m(\omega)$ is so narrow that it does not overlap with the other Lorentzians $T_{m'}(\omega)$. With this result we can now write the coupling strength (6) in the form:

$$\eta_\omega = \sum_{m=-\infty}^{\infty} i \sqrt{\frac{\omega}{\hbar\epsilon_0\ell_c\mathcal{A}}} d e^{i\frac{\omega}{c}\ell_c} \sin\left[\frac{\omega}{c}(x_A + \ell_c)\right] \sqrt{\frac{\Gamma_m}{2\pi}} \frac{1}{(\omega - \tilde{\omega}_m) + i\frac{\Gamma_m}{2}}, \quad (19)$$

which describes the coupling between the global electric field with the atom localized between the mirrors. The product $\ell_c\mathcal{A}$ appearing in the coupling strength can be interpreted as the cavity mode volume. In the high- Q case considered here, it happens to be identical to the mode volume determined by the geometric parameters of the cavity: its mirror separation (or geometric length, ℓ_c), and mirror area, \mathcal{A} . However, we emphasise that the mode volume was not introduced by normalizing the field in a perfect resonator of length ℓ_c . Instead, it is a result of the finite width of the resonances in Eq. (15). To this respect, recovering ℓ_c has been a coincidence. In many cases this does not prevail, which shall be demonstrated in the following discussion.

C. Multilayered stack

We now extend our discussion to consider an alternating stack of two dielectric materials. The first layer has a width δ and a refractive index n_1 , with the other a width α and a refractive index n_2 . The stack has $2N - 1$ layers:

$N - 1$ pairs of dielectric and one additional layer of index n_1 . As such, the first and last layers of the stack have the higher refractive index ($n_1 > n_2$)[26]. We do not include in our model a substrate on which the dielectric coating is deposited, which would normally correspond to a final, significantly thicker, layer of low index material. An updated cavity model is shown in Fig. 2 and the corresponding relative permittivity is given by:

$$\epsilon_r(x) = \begin{cases} 1 & -\ell_c < x \leq 0 \\ n_1^2 & j_1(\delta + \alpha) < x \leq j_1(\delta + \alpha) + \delta \\ n_2^2 & (j_2 - 1)(\delta + \alpha) + \delta < x \leq j_2(\delta + \alpha) \\ 1 & x > N(\delta + \alpha) - \alpha \end{cases}, \quad (20)$$

where $j_1 \in \{0, 1, 2, \dots, N - 1\}$ and $j_2 \in \{1, 2, \dots, N - 1\}$. The cavity is designed such that its fundamental longitudinal mode is at wavelength λ_0 , which is also used to specify the quarter wave dielectric layer optical thickness: $\delta = \lambda_0/4n_1$ and $\alpha = \lambda_0/4n_2$. For simplicity, we further consider $n_2 = 1$. Again, by following the continuity of the field and its derivative, we solve Helmholtz equation (2) and find that the mode can be described in terms of the following functions:

$$B_0(\omega, x) = e^{i\frac{\omega}{c}(x+\ell_c)},$$

$$B_j(\omega, x) = \begin{cases} \frac{1}{1-r_1} (B_{j-1}(\omega, x_2(j)) + r_1 B_{j-1}^*(\omega, x_2(j))) e^{i\frac{\omega}{c}(x-x_2(j))} & j \text{ even,} \\ \frac{1}{1+r_1} (B_{j-1}(\omega, x_1(j)) - r_1 B_{j-1}^*(\omega, x_1(j))) e^{i\frac{\omega}{c}n_1(x-x_1(j))} & j \text{ odd,} \end{cases}$$

where

$$x_1(j) = \frac{j-1}{2}(\delta + \alpha),$$

$$x_2(j) = \frac{j}{2}(\delta + \alpha) - \alpha.$$

The solution to the Helmholtz equation is then given by

$$\Phi_\omega(x) = \sum_{j=0}^{2N} CA_j(\omega, x) \chi_{\Omega_j}, \quad (21)$$

where j runs over the $2N - 1$ possible layers, labelled as $\Omega_j \subset \mathbb{R}$. The $2N$ th term describes the mode exiting the cavity. C is a normalization factor common to all terms and

$$A_j(\omega, x) = B_j(\omega, x) - B_j^*(\omega, x).$$

In particular, Ω_j has the form

$$\Omega_0 = [-\ell_c, 0],$$

$$\Omega_j = \begin{cases} [x_2(j), x_2(j) + \alpha], & j \text{ even,} \\ [x_1(j), x_1(j) + \delta], & j \text{ odd.} \end{cases}$$

Here $A_0(\omega, x)$ corresponds to the mode propagating between the two mirrors and $A_{2N}(\omega, x)$ is the mode corresponding to the outgoing wave.

For a mismatch of the light propagation frequency, ω , with the stack design frequency, $\omega_0 = 2\pi c/\lambda_0$, the intensity of the mode can either decay or grow exponentially through the stack. This can potentially be a combination of each, achieving extremal points of intensity within the dielectric-layer stack. Some examples are shown in Fig. 3.

D. Effective cavity response function

After a mode has been described in the form of Eq. (21), it is important to consider an effective transmissivity, reflectivity and response for a multilayered cavity, resembling Eq. (9). Following the normalization of the modes in (21), the description of the inside and outside modes have the form

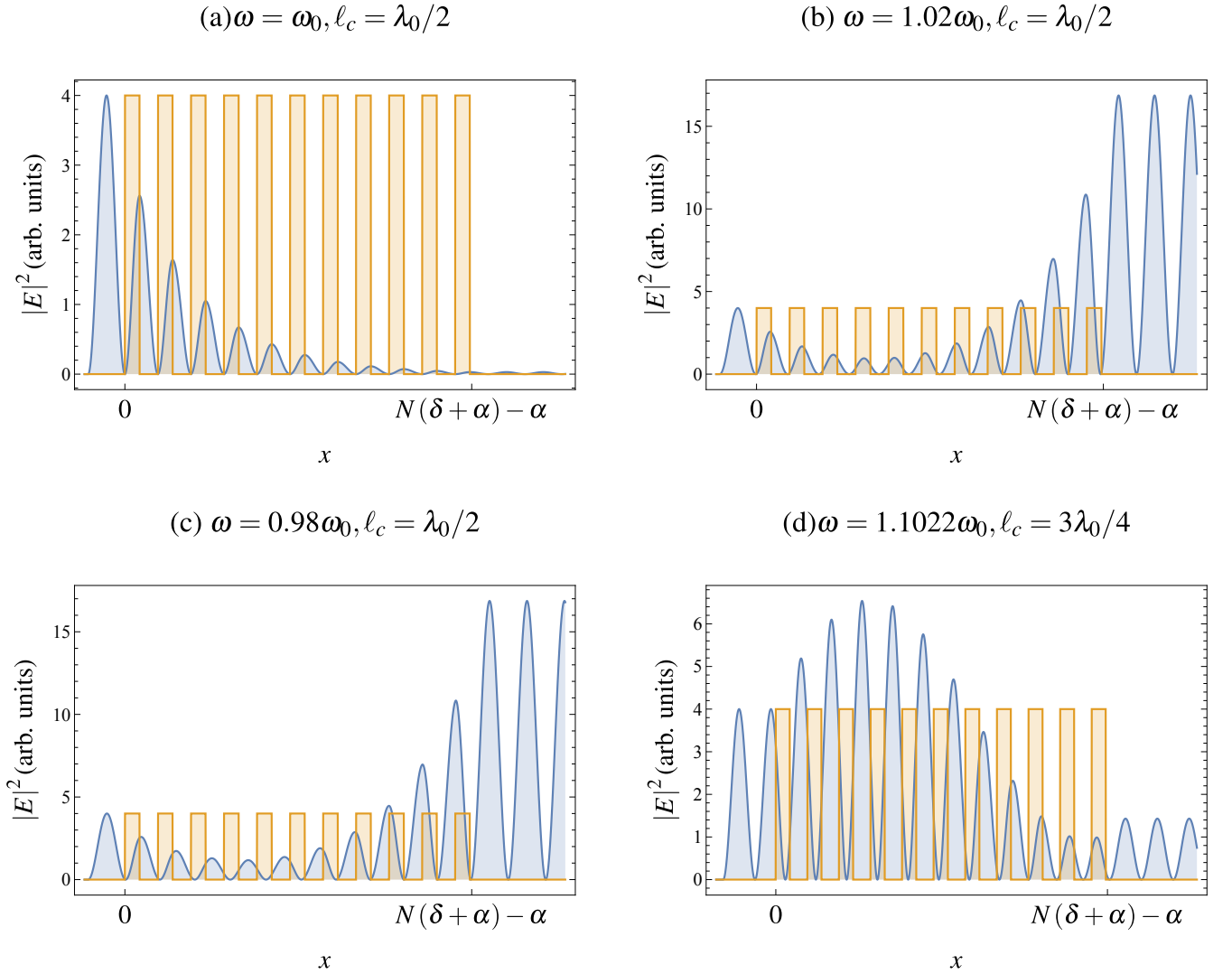


FIG. 3: Mode propagation of a wave of wavelength λ , for a cavity with a multilayered stack with an index of $n_1 = 1.25$. A perfect mirror stands at $x = -\ell_c$, forming a cavity of length ℓ_c with an alternating dielectric stack of 21 alternating layers of width $\delta = \lambda_0/4n_1$ and $\alpha = \lambda_0/4n_2$ (n_2 is taken to be 1). The propagation frequency $\omega = 2\pi c/\lambda$ is varied to observe the mode propagation. In (a), the case when $\ell_c = \lambda_0/2$ and ω exactly matches with the cavity design resonance frequency ω_0 is shown, obtaining the strongest confinement of light inside of the cavity. In (b) and (c), we can see how the intensity changes when the propagating light is slightly off resonance. Finally, in (d) we increase the cavity length to reach $\ell_c = 3\lambda_0/4$ and observe that we achieve resonance coupling when $\omega = 1.1022\omega_0$. Moreover, we can see that in this case the intensity of the light within the layer stack exceeds the intensity of the light inside of the cavity.

$$\begin{aligned}\Phi_{\omega,\text{in}}(x) &= 2ie^{i\frac{\omega}{c}\ell_c}\mathcal{T}(\omega)\sin\left[\frac{\omega}{c}(x+\ell_c)\right], \\ \Phi_{\omega,\text{out}}(x) &= e^{2i\frac{\omega}{c}\ell_c}\frac{\mathcal{T}(\omega)}{\mathcal{T}^*(\omega)}e^{i\frac{\omega}{c}x} - e^{-i\frac{\omega}{c}x}.\end{aligned}$$

Here, $\mathcal{T}(\omega)$ is the field amplitude ratio of the multilayered cavity, which has the form

$$\mathcal{T}(\omega) = \frac{e^{-i\frac{\omega}{c}(\ell_c+(N-1)(\delta+\alpha))}}{B_{2N-2}^*(\omega)} \frac{t(\omega)}{1 + e^{i\frac{\omega}{c}\delta}e^{i\phi_B(\omega)}r(\omega)}, \quad (22)$$

where $\phi_B(\omega) = \arg(B_{2N-2}/B_{2N-2}^*)$ and for simplicity we omitted the argument of $B_{2N-2} = B_{2N-2}(\omega, x_1(2N-1))$. Here, $t(\omega)$ and $r(\omega)$ remain the same as for the single layer case.

If we introduce an indexing of the response function defined above, such that $\mathcal{T}(\omega) = \mathcal{T}_N(\omega)$, where the label N stands for the $2N - 1$ layers, then it can be shown that

$$\frac{e^{-i\frac{\omega}{c}(\ell_c + (N-1)(\delta + \alpha))}}{B_{2N-2}^*(\omega)} = \mathcal{T}_{N-1}(\omega),$$

where $\mathcal{T}_{N-1}(\omega)$ is the response function of a cavity having a dielectric stack with $2N - 3$ dielectric layers. Fig. 4 shows a series of different cavity response functions for different numbers of layer stacks and cavity lengths. Here, our model is seen to exhibit the standard behavior of an optical cavity by showing a decreased linewidth as the number of layers increases, as would be expected from increased mirror reflectivity. Further, the free spectral range of the cavity clearly decreases as its length is increased.

Just as in the case of the single-layered cavity, we can also write the square modulus of the response function as a sum of Lorentzian-like functions, analogous to the one in Eq. (13):

$$|\mathcal{T}(\omega)|^2 = \sum_{m=-\infty}^{\infty} \frac{c}{\delta |B_{2N-2}(\omega)|^2} \frac{\gamma_N(\omega)}{(\omega - \tilde{\omega}_m(\omega))^2 + \left(\frac{\gamma_N(\omega)}{2}\right)^2}, \quad (23)$$

where

$$\begin{aligned} \gamma_N(\omega) &= -c \frac{\ln |r(\omega)|}{\delta/2}, \\ \tilde{\omega}_m &= \frac{c\pi}{\delta/2} m - c \frac{(\phi_r(\omega) + \phi_B(\omega) + \pi)}{\delta}. \end{aligned}$$

The term $\phi_B(\omega)$ in the expression of $\tilde{\omega}_m$ accounts for the multilayer nature of the mirror. In the single-layered case, this has the simple, analytical form $\phi_{B_1}(\omega) = 2\ell_c\omega/c$, which leads to the expressions in Eq. (14).

As we can see from Fig. 4, the multilayer structure leads to a narrowly peaked Lorentzian response function. In order to obtain the individual Lorentzians corresponding to each peak in the response function, we apply the following approximation:

$$|\mathcal{T}(\omega)|^2 \approx \sum_m \frac{c}{2L_N^{(m)}} \frac{\gamma_N^{(m)}}{\left(\omega - \omega_N^{(m)}\right)^2 + \left(\frac{\gamma_N^{(m)}}{2}\right)^2}, \quad (24)$$

where $L_N^{(m)}$, $\gamma_N^{(m)}$ and $\omega_N^{(m)}$ are parameters that are found numerically when we fit each individual peak to the exact cavity response function shown in Eq. (23). In the case of a single-layered mirror, we obtain the individual Lorentzians by evaluating the parameters in (14) at the resonance frequencies $\tilde{\omega}_m$. Here, however, we cannot follow the same procedure due to the complicated nature of the coefficient $|B_{2N-2}(\omega)|^2$. Therefore, we apply a numerical fitting to recover the accuracy of the procedure described above.

We will now examine what happens when we vary the spacing between the mirrors. By taking into account the multilayer structure of the mirror, we also observe resonance frequency shifts from the expected resonances, i.e. for a cavity having a mirror spacing ℓ_c , the expected resonance frequency would be $\omega_m = 2\pi c/\lambda_m = \pi m (c/\ell_c)$, where m is the number of antinodes between the mirrors. However, the resonance frequencies that we obtain with a multilayered structure, in general, do not match the values of ω_m described above (see Fig. 5). In other words, if in the multilayered case we write $\omega_{\text{eff}} = \omega_N^{(m)} = \pi m (c/\ell_{\text{eff}})$ for the resonance frequencies, then, in general ℓ_{eff} is different from ℓ_c . In particular, only whenever we have $\ell_c = p\lambda_0/2$, where p is an integer number, then ℓ_{eff} is the same as ℓ_c . Moreover, the shorter the cavity, the greater the difference between ω_{eff} and ω_m .

Each term in Eq. (24) corresponds to a well separated single Lorentzian at a resonance frequency $\omega_N^{(m)}$, hence for the response function we can write

$$\mathcal{T}(\omega) \approx \sum_m \sqrt{\frac{c}{2L_N^{(m)}}} \frac{\sqrt{\gamma_N^{(m)}}}{\left(\omega - \omega_N^{(m)}\right) + i\frac{\gamma_N^{(m)}}{2}} = \sum_m \mathcal{T}_m(\omega), \quad (25)$$

Unlike the single layer case, this expression for the response function is general; being applicable to cavities of any length, dielectric layer number and refractive index n_1 . It is now possible to write the coupling strength (6) for this case:

$$\eta_\omega = \sum_{m=-\infty}^{\infty} i \sqrt{\frac{\omega}{\hbar\epsilon_0 L_N^{(m)} \mathcal{A}}} d e^{i\frac{\omega}{c}\ell_c} \sin\left[\frac{\omega}{c}(x_A + \ell_c)\right] \sqrt{\frac{\gamma_N^{(m)}}{2\pi}} \frac{1}{\left(\omega - \omega_N^{(m)}\right) + i\frac{\gamma_N^{(m)}}{2}}. \quad (26)$$

If we compare this result with the single-layer case of Eq. (19), we can see that the expressions are the same, with the exception that for the multilayer case we have $L_N^{(m)}$ instead of ℓ_c and $\gamma_N^{(m)}$ instead of Γ_m . Similarly, if we interpret the product $L_N^{(m)} \mathcal{A}$ in the pre-factor as the mode volume, it is no longer defined through the geometric length of the cavity, due to the discrepancy between $L_N^{(m)}$ and ℓ_c .

Over the width $\gamma_N^{(m)}$ of a single Lorentzian, ω is close to $\omega_N^{(m)}$ and varies very slowly, therefore we can further approximate the mode selective coupling $\eta_{\omega,m}$ as:

$$\eta_{\omega,m} \approx i \sqrt{\frac{\omega_N^{(m)}}{\hbar\epsilon_0 L_N^{(m)} \mathcal{A}}} d e^{i\frac{\omega}{c}\ell_c} \sin\left[\frac{\omega}{c}(x_A + \ell_c)\right] \sqrt{\frac{\gamma_N^{(m)}}{2\pi}} \frac{1}{\left(\omega - \omega_N^{(m)}\right) + i\frac{\gamma_N^{(m)}}{2}}. \quad (27)$$

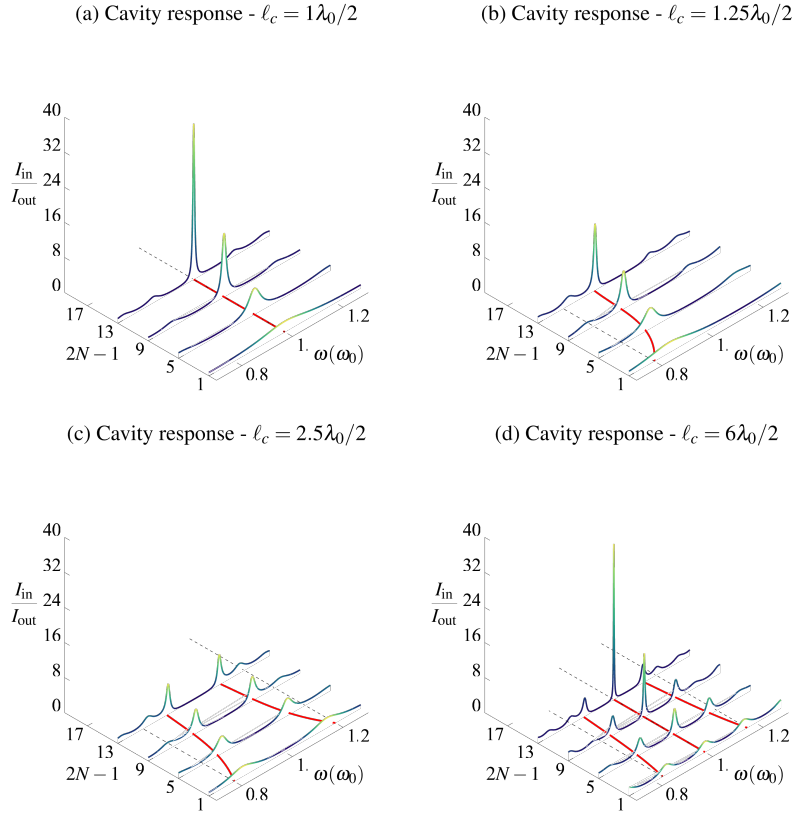


FIG. 4: Cavity inside-outside intensity ratio, $I_{\text{in}}/I_{\text{out}}$, as a function of the angular frequency of the light and the number of layers, $2N - 1$, for a cavity with a multilayered stack with a refractive index $n_1 = 1.25$. A perfect mirror stands at $x = -\ell_c$, and there is an alternating dielectric stack with a varying number of N layers of width $\delta = \lambda_0/4n_1$ and $N - 1$ layers of width $\alpha = \lambda_0/4n_2$ (where n_2 is taken to be 1). Both the number of dielectric layers and the spacing of the cavity are varied to observe different sorts of cavity response functions. All of these can be decomposed as a sum of Lorentzian functions in ω . The dashed lines correspond to cavity classical resonances: $\omega_m = m\pi c/\ell_c$, where m is the number of antinodes between the mirrors. The red, solid lines correspond to ω_{eff} , the peak responses followed by the modes. These do not coincide with ω_m and are strongly dependent on the number of layers.

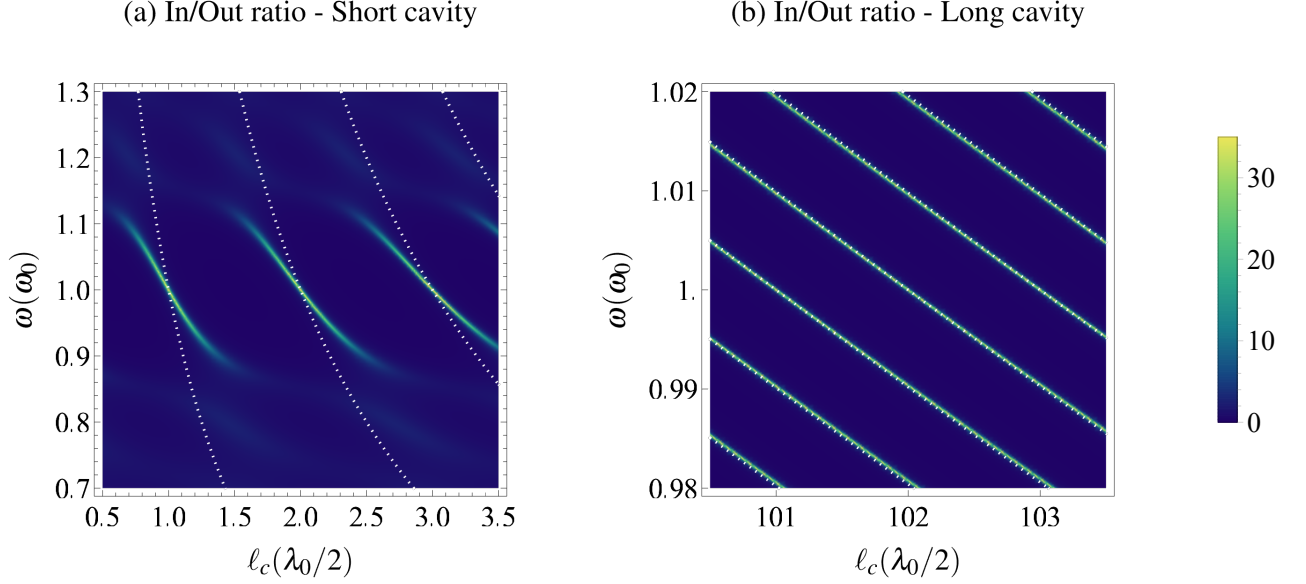


FIG. 5: Calculated Inside/Outside intensity ratio using the electromagnetic propagation of the mode versus $\pi mc/\ell_c$ shown in white, dotted lines. When cavities are very short, the mismatch is appreciable and the maximum inside/outside ratio lines predicted classically differ significantly with respect to the mode prediction. We can see that, only at the points where we have a cavity of length $\ell_c = p\lambda_0/2$, where p is an integer, the predicted and actual lines match.

IV. EFFECTIVE HAMILTONIAN AND ATOM-CAVITY COUPLING

In section II we derived a Hamiltonian describing the global closed system consisting of an atom, cavity and environment. In this section, our goal is to extract an effective Hamiltonian to describe the dynamics of the open atom-cavity system.

In further analysis, we limit the Hilbert space to a subspace containing the excited atom state $|e, 0\rangle$ and the single excitation of the cavity in a superposition of frequency modes: $|g, 1\rangle$. To write the effective Hamiltonian for such a system we define the following operator:

$$\hat{a}_m = \frac{1}{g_m} \int_0^\infty d\omega \eta_{\omega,m} \hat{a}(\omega), \quad (28)$$

which satisfies the commutation relations:

$$\begin{aligned} [\hat{a}_m, \hat{a}_{m'}^\dagger] &= \delta_{mm'}, \\ [\hat{a}_m, \hat{a}_{m'}] &= 0. \end{aligned}$$

The definition (28) allows one to transform the continuous model (7) into discrete one.

It can be shown that g_m is a normalization constant given by (see Appendix B):

$$g_m = i \sqrt{\frac{\omega_N^{(m)}}{\hbar \epsilon_0 L_N^{(m)} \mathcal{A}}} d e^{i \frac{\omega_N^{(m)}}{c} \ell_c} \sin \left[\frac{\omega_N^{(m)}}{c} (x_A + \ell_c) \right] + \mathcal{O}(\epsilon^2), \quad (29)$$

up to an error of the order ϵ^2 , where $\epsilon = \gamma_N^{(m)} \frac{x_A + \ell_c}{c}$. The width $\gamma_N^{(m)}$ decreases with a greater number of layers and cavity length, hence ϵ becomes smaller (see Fig. 4) and the approximation is well validated.

Assuming that only one of the cavity modes at $\omega_N^{(m)}$ is close to the resonance frequency ω_A of the atom, all other modes can be safely disregarded and the effective Hamiltonian then reads (see Appendix B):

$$\hat{H}_{\text{eff}} = \hbar \omega_A \hat{\sigma}_+ \hat{\sigma}_- + \left(\hbar \omega_N^{(m)} - i \hbar \frac{\gamma_N^{(m)}}{2} \right) \hat{a}_m^\dagger a_m + i \hbar g_m \hat{\sigma}_+ \hat{a}_m - i \hbar g_m^* \hat{\sigma}_- \hat{a}_m^\dagger, \quad (30)$$

where $\omega_N^{(m)} - \omega_A \ll \omega_N^{(m)}$, g_m is the coupling of a single cavity mode $\omega_N^{(m)}$ with the atom and $\gamma_N^{(m)}$ is the width of Lorentzian centered at the resonance frequency $\omega_N^{(m)}$.

The expression (29) looks similar to the atom-cavity coupling for a perfect cavity, i.e., if we write the perfect cavity Hamiltonian with zero boundary conditions at the mirrors we obtain:

$$g_m = i\sqrt{\frac{\omega_m}{\hbar\epsilon_0\ell_c\mathcal{A}}}d e^{i\frac{\omega_m}{c}\ell_c} \sin\left[\frac{\omega_m}{c}(x_A + \ell_c)\right], \quad (31)$$

which is different from (29) by an error factor $\mathcal{O}(\epsilon^2)$, and again due to the mismatch between ℓ_c and $L_N^{(m)}$ and ω_m and $\omega_N^{(m)}$.

For the more general case, when the atom is not necessarily on resonance with the cavity, (i.e. we consider the states $|e, 0\rangle$, $|g, 1\rangle$, as well as $|e, 1\rangle$ and $|g, 0\rangle$), it can be shown that the Hamiltonian (30) becomes:

$$\hat{H}_{\text{eff}} = \hbar\omega_A\hat{\sigma}_+\hat{\sigma}_- + \hbar\sum_m\left(\omega_N^{(m)} - i\frac{\gamma_N^{(m)}}{2}\right)\hat{a}_m^\dagger\hat{a}_m + ig_m\hat{\sigma}_+\hat{a}_m - ig_m^*\hat{\sigma}_-\hat{a}_m^\dagger + i\underline{g}_m\hat{\sigma}_-\hat{a}_m - i\underline{g}_m^*\hat{\sigma}_+\hat{a}_m^\dagger, \quad (32)$$

where

$$\underline{g}_m = i\sqrt{\frac{\omega_N^{(m)}}{\hbar\epsilon_0L_N^{(m)}\mathcal{A}}}d^* e^{i\frac{\omega_N^{(m)}}{c}\ell_c} \sin\left[\frac{\omega_N^{(m)}}{c}(x_A + \ell_c)\right] + \mathcal{O}(\epsilon^2). \quad (33)$$

V. DISCUSSION AND CONCLUSIONS

In this paper we have examined light-matter interaction in optical cavities delimited by multilayered dielectric mirrors using a model where no assumptions over the longitudinal constraints of the field have been made. The analysis of the multilayer structure allowed us to perform a more realistic description of the effective cavity length and corresponding mode volume.

The effective cavity length ℓ_{eff} , as defined in the literature [16, 27, 28], determines the cavity resonance and, as we have shown in this paper, does not correspond to the coupling factor cavity length $L_N^{(m)}$ used for determining the strength of the cavity-matter coupling. We have found that these two lengths do not correspond to each other whenever a multilayer structure is taken into consideration. Additionally, the resonance frequencies through which ℓ_{eff} is defined no longer coincide with the expected resonances at integer multiples of $c/(2\ell_c)$. In other words, ℓ_{eff} is different from the geometric cavity length ℓ_c unless the latter is an integer multiple of $\lambda_0/2$, where λ_0 is the stack design wavelength. A pronounced side effect of this discrepancy is that the most common approach [13] for determining a cavity length by means of measuring its free-spectral range is bound to fail for very short cavities. The geometric length of the cavity might differ by up to $\lambda_0/2$ from its effective length determining the free spectral range. This difference may be of importance in applications where the cavity spacings used are very short and the mirrors are made of dielectric coatings [29, 30].

The standard model for light-matter interaction in optical cavities considers the mode volume of the cavity to be the product between the longitudinal extent of the mode (considered to be only the separation between the mirrors) and a factor accounting for the transverse behavior of the mode [24]. However, here we have shown that this is only valid if the mirrors can be seen as hard mode-delimiting boundaries. Any physical cavity is very different to that respect. The mode penetrates into the dielectric mirror stack, couples to the outside and the light frequency is not quantized in these open systems. However, even though we don't explicitly consider a mode volume, we show that the atom-cavity coupling involves a factor having the unit of volume. Only in the case of a perfect cavity having hard boundaries at the positions of the mirrors, this factor coincides with the geometric definition of the mode volume. In the multilayered case, however, this factor does not necessarily correspond to the geometric volume of the cavity, particularly due to the discrepancy between the geometric length ℓ_c , the effective length ℓ_{eff} and $L_N^{(m)}$. More specifically, for a cavity with a mirror spacing $\ell_c = \lambda_0/2$, the effective cavity length ℓ_{eff} coincides with ℓ_c , however the coupling factor cavity length does not: $L_{19}^{(1)} \approx 3.06\ell_c$. If we increase the mirror spacing, such that $\ell_c = 1.8\lambda_0/2$, then for the other parameters we obtain: $\ell_{\text{eff}} \approx 0.53\ell_c$ and $L_{19}^{(1)} \approx 2.4\ell_c$. As expected, for longer cavities the discrepancy between these terms decreases, e.g., when $\ell_c = 30.8\lambda_0/2$ we obtain $\ell_{\text{eff}} \approx 0.97\ell_c$ and $L_{19}^{(q)} \approx 1.09\ell_c$, where q is the number of the mode with highest amplitude. This discrepancy between the coupling factor cavity length $L_N^{(m)}$ and geometric cavity length ℓ_c can lead to a Purcell factor different from the one calculated by using a standard approach, especially with short mirror spacings.

Eventually, from the general quantized field we extract an effective Hamiltonian describing an open cavity system. From this we explicitly calculate the atom-cavity coupling rate both for on and off resonant behavior. This quantization from first principles of more realistic open cavities is a preliminary step for considering the complex dynamics featuring a laser-driven atom in such cavities. Work is ongoing to derive microscopic models [31] for controlling photonic states produced from such cavities [7].

We also note that submicrometric confinement of light in (dissipative and dispersive) metallic media gives rise to surface plasmon polaritons that can be used for quantum optics at nanoscale [32]. Albeit these are no multilayered structures, the construction of quantized models taking into account the resulting losses follows a similar approach and is based on a microscopic oscillator model for the medium coupled to the electromagnetic field [33] with a particular care for finite-size media [34, 35].

Acknowledgments

J.R.A. acknowledges Christian Poveda regarding code optimization. All authors acknowledge Mark IJspeert, Marwan Mohammed and Ezra Kassa for useful discussions.

Funding

European Union Horizon 2020 (Marie Skłodowska-Curie 765075-LIMQUET).
EPSRC through the quantum technologies programme (NQIT hub, EP/M013243/1).
EIPHI Graduate School (ANR-17-EURE-0002).

-
- [1] J. I. Cirac and H. J. Kimble, *Nature Photonics* **11**, 18 (2017), ISSN 1749-4893.
 - [2] S. Ritter, C. Nölleke, C. Hahn, A. Reiserer, A. Neuzner, M. Uphoff, M. Mücke, E. Figueroa, J. Bochmann, and G. Rempe, *Nature* **484**, 195 (2012), ISSN 0028-0836, 1476-4687.
 - [3] H. J. Kimble, *Nature* **453**, 1023 (2008), ISSN 1476-4687.
 - [4] T. Wilk, S. C. Webster, A. Kuhn, and G. Rempe, *Science* **317**, 488 (2007), ISSN 0036-8075, 1095-9203.
 - [5] D. L. Moehring, P. Maunz, S. Olmschenk, K. C. Younge, D. N. Matsukevich, L.-M. Duan, and C. Monroe, *Nature* **449**, 68 (2007), ISSN 1476-4687.
 - [6] T. D. Barrett, A. Rubenok, D. Stuart, O. Barter, A. Holleczeck, J. Dille, P. B. R. Nisbet-Jones, K. Poulios, G. D. Marshall, J. L. O'Brien, et al., *Quantum Science and Technology* **4**, 025008 (2019), ISSN 2058-9565.
 - [7] A. Kuhn, M. Hennrich, T. Bondo, and G. Rempe, *Applied Physics B* **69**, 373 (1999).
 - [8] M. Keller, B. Lange, K. Hayasaka, W. Lange, and H. Walther, *Nature* **431**, 1075 (2004), ISSN 1476-4687.
 - [9] S. Johnson, P. R. Dolan, T. Grange, A. A. P. Trichet, G. Hornecker, Y. C. Chen, L. Weng, G. M. Hughes, A. A. R. Watt, A. Auffèves, et al., *New J. Phys.* **17**, 122003 (2015), ISSN 1367-2630.
 - [10] X. Ding, Y. He, Z.-C. Duan, N. Gregersen, M.-C. Chen, S. Unsleber, S. Maier, C. Schneider, M. Kamp, S. Höfling, et al., *Phys. Rev. Lett.* **116**, 020401 (2016).
 - [11] E. Purcell, *Physical Review* **69**, 681, B10 (1946), ISSN 0031-899X.
 - [12] H. J. Kimble, *Phys. Scr.* **1998**, 127 (1998), ISSN 1402-4896.
 - [13] B. E. Saleh and M. C. Teich, *Fundamentals of Photonics*, vol. 22 (John Wiley & Sons, 1991).
 - [14] H. A. Macleod, *Thin-Film Optical Filters* (Institute of Physics Publishing, 2018), ISBN 978-1-315-27049-4 978-1-351-98222-1.
 - [15] A. M. Kern, D. Zhang, M. Brecht, A. I. Chizhik, A. V. Failla, F. Wackenhut, and A. J. Meixner, *Chem. Soc. Rev.* **43**, 1263 (2014), ISSN 1460-4744.
 - [16] P. Zhong, W. Rong-han, and W. Qi-ming, *Acta Physica Sinica (Overseas Edition)* **4**, 810 (1995), ISSN 1004-423X.
 - [17] J. H. Apfel, *Applied Optics* **16**, 1880 (1977), ISSN 0003-6935, 1539-4522.
 - [18] K. J. Vahala, *Nature* **424**, 839 (2003), ISSN 1476-4687.
 - [19] W. Vogel and D.-G. Welsch, *Quantum Optics* (Wiley, 2006), 1st ed., ISBN 978-3-527-40507-7 978-3-527-60852-2.
 - [20] K. Ujihara, A. Nakamura, O. Manba, and X.-P. Feng, *Jpn. J. Appl. Phys.* **30**, 3388 (1991), ISSN 1347-4065.
 - [21] X.-P. Feng, *Optics Communications* **83**, 162 (1991), ISSN 0030-4018.
 - [22] S. M. Dutra, *Cavity Quantum Electrodynamics: The Strange Theory of Light in a Box*, Wiley Series in Lasers and Applications (Wiley, Hoboken, NJ, 2005), ISBN 978-0-471-44338-4.
 - [23] D. Walls and G. J. Milburn, in *Quantum Optics*, edited by D. Walls and G. J. Milburn (Springer Berlin Heidelberg, Berlin, Heidelberg, 2008), pp. 127–141, ISBN 978-3-540-28574-8.
 - [24] W. T. Silfvast, *Laser Fundamentals* (Cambridge University Press, Cambridge ; New York, 2008), second edition ed., ISBN 978-0-521-54105-3.

- [25] B. Rousseaux, Ph.D. thesis, Laboratoire Interdisciplinaire Carnot de Bourgogne (2016).
- [26] M. Banning, *J. Opt. Soc. Am.* **37**, 792 (1947).
- [27] Y. Suematsu, S. Arai, and K. Kishino, *Journal of Lightwave Technology* **1**, 161 (1983), ISSN 1558-2213.
- [28] L. A. Coldren, S. W. Corzine, and M. L. Mashanovitch, *Diode Lasers and Photonic Integrated Circuits* (Wiley-Blackwell, Hoboken, N.J, 2012), 2nd ed., ISBN 978-0-470-48412-8.
- [29] A. A. P. Trichet, P. R. Dolan, D. James, G. M. Hughes, C. Vallance, and J. M. Smith, *Nano Lett.* **16**, 6172 (2016), ISSN 1530-6984.
- [30] M. Mader, J. Reichel, T. W. Hänsch, and D. Hunger, *Nature Communications* **6**, 7249 (2015), ISSN 2041-1723.
- [31] G. L. Giorgi, A. Saharyan, S. Guérin, D. Sugny, and B. Bellomo, *Phys. Rev. A* **101**, 012122 (2020).
- [32] D. E. Chang, A. S. Sørensen, E. A. Demler, and M. D. Lukin, *Nature Physics* **3**, 807 (2007), ISSN 1745-2473.
- [33] B. Huttner and S. M. Barnett, *Physical Review A* **46**, 4306 (1992), ISSN 1050-2947.
- [34] V. Dorier, J. Lampart, S. Guérin, and H. R. Jauslin, *Physical Review A* **100** (2019), ISSN 2469-9926.
- [35] V. Dorier, S. Guérin, and H.-R. Jauslin, *Nanophotonics* **9**, 3899 (2020), ISSN 2192-8614.

Appendix A: Lorentzian structure of the cavity spectral response function

In this Appendix we derive the Lorentzian structure of the cavity response function (10) [22]:

$$T(\omega) = \frac{t(\omega)}{1 + r(\omega)e^{2i\frac{\omega}{c}L_1}}. \quad (\text{A1})$$

Writing the square modulus of $T(\omega)$, and using conditions (11) and (12) we get

$$|T(\omega)|^2 = \frac{1 - |r|^2}{|1 + |r|e^{i\Phi}|^2} = \left[1 - \frac{|r|e^{i\Phi}}{1 + |r|e^{i\Phi}} - \frac{|r|e^{-i\Phi}}{1 + |r|e^{-i\Phi}} \right],$$

where for simplicity we have not written the dependence of $r(\omega)$ on ω , and we have used the following notations $r(\omega) = |r|e^{i\Phi_r(\omega)}$, $\Phi = 2\frac{\omega}{c}L_1 + \Phi_r(\omega)$. Using the geometric series formula

$$\sum_{n=1}^{+\infty} q^n = \frac{q}{1 - q}, \quad |q| < 1$$

we can write the above expression for the response function as follows

$$\begin{aligned} |T(\omega)|^2 &= 1 + \sum_{n=1}^{+\infty} |r|^n \left(e^{in(\Phi+\pi)} + e^{-in(\Phi+\pi)} \right) \\ &= \sum_{n=-\infty}^{+\infty} |r|^{|n|} e^{in(\Phi+\pi)}. \end{aligned}$$

We further apply the Poisson summation formula, which states

$$\sum_{n=-\infty}^{+\infty} f(n) = \sum_{m=-\infty}^{+\infty} \int_{-\infty}^{+\infty} dx f(x) e^{-i2\pi mx} = \sum_{m=-\infty}^{+\infty} \tilde{f}(m)$$

where $\tilde{f}(m) = \mathbf{F}_m[f(x)]$ is the Fourier transform of $f(x)$. We apply the Fourier transform to the function

$$f(x) = |r|^{|x|} e^{ix(\Phi+\pi)} = e^{|x| \ln |r| + ix(\Phi+\pi)}$$

and obtain

$$\mathbf{F}_m[f(x)] = \frac{2a}{a^2 + \alpha^2},$$

where $a = -\ln |r|$, $\alpha = \Phi + \pi - 2\pi m$. Hence,

$$\tilde{f}(m) = \frac{-2 \ln |r|}{(\ln |r|)^2 + ((\Phi + \pi) - 2\pi m)^2}.$$

We further expand this expression by writing the explicit expression for Φ :

$$\tilde{f}(m) = \frac{-2 \ln |r|}{(\ln |r|)^2 + ((2\frac{\omega}{c}L_1 + \Phi_r + \pi) - 2\pi m)^2},$$

and multiplying both the numerator and the denominator by $(c/2L_1)^2$ we find the Lorentzian structure of the cavity spectral response function, still having the parameters $\tilde{\omega}_m$ and γ_1 depend on ω :

$$\begin{aligned} |T(\omega)|^2 &= \sum_{n=-\infty}^{+\infty} \frac{c}{2L_1} \frac{\gamma_1(\omega)}{(\omega - \tilde{\omega}_m(\omega))^2 + \left(\frac{\gamma_1(\omega)}{2}\right)^2}, \\ \gamma_1(\omega) &= -\frac{c}{L_1} \ln |r(\omega)|, \\ \tilde{\omega}_m &= \frac{\pi c}{L_1} m - \frac{c}{2L_1} (\Phi_r(\omega) + \pi), \end{aligned}$$

In the limit of large refractive indices, the reflection coefficient becomes $r(\omega) = r_1 e^{-i(\pi + \frac{\omega}{c}\delta)}$, i.e $\Phi_r(\omega) = -(\pi + \frac{\omega}{c}\delta)$, which tends to $-\pi$ in the limit of a negligible width δ of the dielectric, and we recover the expression for a perfect cavity.

Appendix B: Effective Hamiltonian

In order to extract the description of the atom-cavity open system from the one described in section II, we first solve the Schrödinger equation

$$i\hbar \frac{\partial}{\partial t} |\psi(t)\rangle = \hat{H} |\psi(t)\rangle. \quad (\text{B1})$$

If we put the Hamiltonian (7) and the following wavefunction

$$|\psi(t)\rangle = \int_0^{+\infty} d\omega e^{-i\omega t} c_{g,1}(\omega, t) |g, 1\rangle + e^{-i\omega_A t} c_{e,0}(t) |e, 0\rangle \quad (\text{B2})$$

into Eq. (B1), we obtain the dynamical equations for the coefficients $c_{g,1}(\omega, t)$, $c_{e,0}(t)$ [25]:

$$\dot{c}_{g,1}(\omega, t) = - \sum_m \eta_{\omega,m}^* e^{i(\omega-\omega_A)t} c_{e,0}(t) \quad (\text{B3})$$

$$\dot{c}_{e,0}(t) = \int_0^{+\infty} d\omega \sum_m \eta_{\omega,m} e^{-i(\omega-\omega_A)t} c_{g,1}(\omega, t) \quad (\text{B4})$$

In order to trace out the continuous degrees of freedom from the dynamics, we define the integrated, mode-selective probability amplitude:

$$c_{g,1}^{(m)}(t) = \frac{1}{g_m} \int_0^{+\infty} d\omega \eta_{\omega,m} e^{-i(\omega-\omega_A)t} c_{g,1}(\omega, t). \quad (\text{B5})$$

We now write the time derivative of this quantity, using the property

$$\eta_{\omega,m}^* \eta_{\omega,m'} = \delta_{mm'} |\eta_{\omega,m}|^2,$$

which is a consequence of the fact that the response function is a sum of narrow peaked and well separated Lorentzians. Using this property we get the equation of motion for the m -th mode, using the integration of (B3) and inverting the order of time and frequency integration:

$$\begin{aligned} \dot{c}_{g,1}^{(m)}(t) &= \dot{c}_{g,1}^{(m,0)}(t) - \frac{1}{g_m} \int_0^{+\infty} d\omega |\eta_{\omega,m}|^2 c_{e,0}(t) \\ &\quad + \frac{i}{g_m} \int_0^t dt' c_{e,0}(t') \int_0^{+\infty} d\omega |\eta_{\omega,m}|^2 (\omega - \omega_A) e^{-i(\omega-\omega_A)(t-t')} \end{aligned} \quad (\text{B6})$$

where we introduce the time derivative of the initial time defined as follows:

$$c_{g,1}^{(m,0)} = \frac{1}{g_m} \int_0^{+\infty} d\omega \eta_{\omega,m} e^{-i(\omega-\omega_A)t} c_{g,1}(\omega, 0).$$

Two integrals appear in (B6):

$$\begin{aligned} \mathcal{I}_1 &= \int_0^{+\infty} d\omega |\eta_{\omega,m}|^2, \\ \mathcal{I}_2 &= \int_0^{+\infty} d\omega |\eta_{\omega,m}|^2 (\omega - \omega_A) e^{-i(\omega-\omega_A)(t-t')}, \end{aligned}$$

which can be evaluated using complex contour methods, and in the limit of $\epsilon = \gamma_N^{(m)} \frac{x_A + \ell}{c} \ll 1$, we obtain (here after in the parameters $\gamma_N^{(m)}$, $L_N^{(m)}$ and $\omega_N^{(m)}$ we omit the index indicating the number of layers)

$$\begin{aligned} \mathcal{I}_1 &= \frac{\omega^{(m)} |d|^2}{\hbar \epsilon_0 \mathcal{A} L^{(m)}} \sin^2 \left[2 \frac{\omega^{(m)}}{c} (x_A + \ell_c) \right], \\ \mathcal{I}_2 &= \frac{\omega^{(m)} |d|^2}{\hbar \epsilon_0 \mathcal{A} L^{(m)}} \sin^2 \left[2 \frac{\omega^{(m)}}{c} (x_A + \ell_c) \right] \left(\Delta_m - i \frac{\gamma^{(m)}}{2} \right) e^{-i(\Delta_m - i \frac{\gamma^{(m)}}{2})(t-t')}, \end{aligned}$$

where $\Delta_m = \omega^{(m)} - \omega_A$. We note that, since we defined g_m as the normalization coefficient of (B5), then the integrals \mathcal{I}_1 and \mathcal{I}_2 become

$$\begin{aligned}\mathcal{I}_1 &= |g_m|^2, \\ \mathcal{I}_2 &= |g_m|^2 \left(\Delta_m - i \frac{\gamma^{(m)}}{2} \right) e^{-i(\Delta_m - i \frac{\gamma^{(m)}}{2})(t-t')},\end{aligned}$$

with

$$g_m = i \sqrt{\frac{\omega^{(m)}}{\hbar \epsilon_0 \mathcal{A} L^{(m)}}} d e^{i \frac{\omega^{(m)}}{c} \ell_c} \sin \left[\frac{\omega^{(m)}}{c} (x_A + \ell_c) \right] + \mathcal{O}(\epsilon^2).$$

Having obtained the expression for g_m , we can now rewrite the dynamical equation (B6) as follows:

$$\begin{aligned}\dot{c}_{g,1}^{(m)} &= \dot{c}_{g,1}^{(m,0)} - g_m^* c_{e,0}(t) \\ &\quad + i g_m^* \int_0^t dt' c_{e,0}(t') \left(\Delta_m - i \frac{\gamma^{(m)}}{2} \right) e^{-i(\Delta_m - i \frac{\gamma^{(m)}}{2})(t-t')}\end{aligned}\tag{B7}$$

If we formally integrate equation (B3) and put the result in (B5), it can be shown that

$$c_{g,1}^{(m)}(t) - c_{g,1}^{(m,0)} = -g_m^* \int_0^t dt' c_{e,0}(t') e^{-i(\Delta_m - i \frac{\gamma^{(m)}}{2})(t-t')},$$

hence Eq. (B7) becomes

$$\dot{c}_{g,1}^{(m)} = \dot{c}_{g,1}^{(m,0)}(t) - g_m^* c_{e,0}(t) - i \left(\Delta_m - i \frac{\gamma^{(m)}}{2} \right) (c_{g,1}^{(m)}(t) - c_{g,1}^{(m,0)}(t)).$$

Considering that at initial time $t = 0$ the atom is in its excited state and there is no photon in the cavity, we finally get the following set of dynamical equations

$$\begin{aligned}\dot{c}_{g,1}^{(m)} &= -g_m^* c_{e,0}(t) - i \left(\Delta_m - i \frac{\gamma^{(m)}}{2} \right) c_{g,1}^{(m)} \\ \dot{c}_{e,0} &= \sum_m g_m c_{g,1}^{(m)}(t),\end{aligned}\tag{B8}$$

which then yields that for the state described by the wavefunction

$$|\psi(t)\rangle = \sum_m c_{g,1}^{(m)} |g, 1_\omega\rangle + c_{e,0}(t) |e, 0\rangle$$

the Hamiltonian can be written as

$$\hat{H}_{\text{eff}} = \hbar \sum_m \left(\Delta_m - i \frac{\gamma^{(m)}}{2} \right) \hat{a}_m^\dagger \hat{a}_m + i g_m \hat{\sigma}_+ \hat{a}_m - i g_m^* \hat{\sigma}_- \hat{a}_m^\dagger.$$

Finally, we can write the effective Hamiltonian back from the rotating frame, via the transformation:

$$R = e^{i \omega_A t (\hat{\sigma}_+ \hat{\sigma}_- + \sum \hat{a}_m^\dagger \hat{a}_m)},$$

leading to an effective Hamiltonian describing the dynamics restricted between the mirrors:

$$\hat{H}_{\text{eff}} = \hbar \omega_A \hat{\sigma}_+ \hat{\sigma}_- + \hbar \sum_m \left(\omega^{(m)} - i \frac{\gamma^{(m)}}{2} \right) \hat{a}_m^\dagger \hat{a}_m + i g_m \hat{\sigma}_+ \hat{a}_m - i g_m^* \hat{\sigma}_- \hat{a}_m^\dagger.\tag{B9}$$

It can be shown that in the case where we have off-resonant atom-cavity coupling, the effective Hamiltonian can be written as follows

$$\hat{H}_{\text{eff}} = \hbar \omega_A \hat{\sigma}_+ \hat{\sigma}_- + \hbar \sum_m \left(\omega^{(m)} - i \frac{\gamma^{(m)}}{2} \right) \hat{a}_m^\dagger \hat{a}_m + i g_m \hat{\sigma}_+ \hat{a}_m - i g_m^* \hat{\sigma}_- \hat{a}_m^\dagger + i \underline{g}_m \hat{\sigma}_- \hat{a}_m - i \underline{g}_m^* \hat{\sigma}_+ \hat{a}_m^\dagger,\tag{B10}$$

where

$$\underline{g}_m = i \sqrt{\frac{\omega^{(m)}}{\hbar \epsilon_0 L^{(m)} \mathcal{A}}} d^* e^{i \frac{\omega^{(m)}}{c} \ell_c} \sin \left[\frac{\omega^{(m)}}{c} (x_A + \ell_c) \right] + \mathcal{O}(\epsilon^2).\tag{B11}$$